

Spin–Orbit Interaction in Solids and Double Groups

The discussion of angular momentum and the rotation group has thus far been limited to integral values of the angular momentum (see Chap. 5). The inclusion of half integral angular momentum states requires the introduction of the spin–orbit interaction and “double groups”, which are the focus of this chapter.

14.1 Introduction

The spin angular momentum of an electron is half integral or $S_z = \hbar/2$. Furthermore, associated with each electron is a magnetic moment $\mu_B = -|e|\hbar/(2mc) = 0.927 \times 10^{-20}$ erg/gauss. The magnetic moment and spin angular momentum for the free electron are related by

$$\boldsymbol{\mu} = -\frac{|e|\hbar}{mc} \mathbf{S} = -\frac{|e|\hbar}{mc} \frac{\mathbf{S}}{2} \frac{2}{|\mathbf{S}|} \quad (14.1)$$

and $\boldsymbol{\mu}$ and \mathbf{S} are oppositely directed because of the negative charge on electrons. This relation between the spin angular momentum and the magnetic moment gives rise to an interaction, called the spin–orbit interaction, which is important in describing the electronic structure of crystalline materials. In this section we briefly review this interaction and then in the following sections of this Chapter, we consider the group theoretical consequences of the half-integral spin and the spin–orbit interaction.

An electron in an atom sees a magnetic field because of its own orbital motion and consequently gives rise to the spin–orbit interaction whereby this internal magnetic field tends to line up its magnetic moment along the magnetic field: $\mathcal{H}_{\text{SO}} = -\boldsymbol{\mu} \cdot \mathbf{H}$. Substitution for $\mathbf{H} = -(\mathbf{v}/c) \times \mathbf{E}$ and $\boldsymbol{\mu} = -[|e|\hbar/(mc)]\mathbf{S}$ together with a factor of 1/2 to make the result correct relativistically yields

$$\mathcal{H}'_{\text{SO}} = \frac{1}{2m^2c^2} (\nabla V \times \mathbf{p}) \cdot \mathbf{S}. \quad (14.2)$$

For an atom the corresponding expression is written as

$$\mathcal{H}'_{\text{SO atom}} = \xi(r)\mathbf{L} \cdot \mathbf{S} \quad (14.3)$$

since $\nabla V \sim \mathbf{r}/r^3$ and where \mathbf{L} is the orbital angular momentum. A detailed discussion of the spin–orbit interaction is found in standard quantum mechanics text books.

This spin–orbit interaction gives rise to a spin–orbit splitting of atomic levels which are labeled by their total angular momentum quantum numbers, as discussed below. As an example, consider an atomic p state ($\ell = 1$). Writing the total angular momentum

$$\mathbf{J} = \mathbf{L} + \mathbf{S}, \quad (14.4)$$

where \mathbf{L} and \mathbf{S} are, respectively, the orbital angular momentum operator and the spin angular momentum operator, we obtain for the dot product

$$\mathbf{J} \cdot \mathbf{J} = (\mathbf{L} + \mathbf{S}) \cdot (\mathbf{L} + \mathbf{S}) = \mathbf{L} \cdot \mathbf{L} + \mathbf{S} \cdot \mathbf{S} + (\mathbf{L} \cdot \mathbf{S} + \mathbf{S} \cdot \mathbf{L}), \quad (14.5)$$

in which the operators \mathbf{L} and \mathbf{S} commute since they operate in different coordinate spaces. Since \mathbf{L} and \mathbf{S} are coupled through the spin–orbit interaction, m_ℓ and m_s are no longer good quantum numbers since they are coupled by \mathcal{H}'_{SO} , though ℓ and s remain good quantum numbers. To find the magnitude of the spin–orbit interaction in (14.2), we need to take the matrix elements of \mathcal{H}'_{SO} in the $|j, \ell, s, m_j\rangle$ representation. Using (14.5) for the operators \mathbf{J} , \mathbf{L} and \mathbf{S} , we obtain for the diagonal matrix element of $\mathbf{J} \cdot \mathbf{J}$

$$j(j+1) = \ell(\ell+1) + s(s+1) + 2\langle \mathbf{L} \cdot \mathbf{S} \rangle / \hbar^2, \quad (14.6)$$

so that the expectation value of $\mathbf{L} \cdot \mathbf{S}$ in the $|j, \ell, s, m_j\rangle$ representation becomes

$$\langle \mathbf{L} \cdot \mathbf{S} \rangle = \frac{\hbar^2}{2} [j(j+1) - \ell(\ell+1) - s(s+1)]. \quad (14.7)$$

For p states with spin–orbit interaction, we have $\ell = 1$, and $s = 1/2$ so that $j = 3/2$ or $1/2$

$$\begin{aligned} \langle \mathbf{L} \cdot \mathbf{S} \rangle &= \hbar^2/2 \quad \text{for } j = 3/2 \\ \langle \mathbf{L} \cdot \mathbf{S} \rangle &= -\hbar^2 \quad \text{for } j = 1/2. \end{aligned} \quad (14.8)$$

Thus the spin–orbit interaction introduces a splitting between the $j = 3/2$ and $j = 1/2$ angular momentum states of the p -levels.

From the expression for the expectation value of $\langle \mathbf{L} \cdot \mathbf{S} \rangle$, we note that the degeneracy of an s -state is unaffected by the spin–orbit interaction, and remains two denoting a spin up and spin down state. On the other hand, a d -state is split up into a $D_{5/2}$ (sixfold degenerate) and a $D_{3/2}$ (fourfold degenerate) state. Thus, the spin–orbit interaction does not lift all the degeneracy of atomic states. To lift the remaining degeneracy, it is necessary to

Table 14.1. Spin-orbit interaction energies for some important cubic semiconductors (for the valence band at $k = 0$) [38, 55]

| semiconductor | atomic number | Γ -point splitting |
|---------------|---------------|-------------------------------|
| diamond | $Z = 6$ | $\Delta E = 0.006 \text{ eV}$ |
| silicon | $Z = 14$ | $\Delta E = 0.044 \text{ eV}$ |
| germanium | $Z = 32$ | $\Delta E = 0.29 \text{ eV}$ |
| InSb | $Z = 49$ | $\Delta E = 0.9 \text{ eV}$ |
| | $Z = 51$ | |

lower the symmetry further, for example, by the application of a magnetic field. The magnitude of the spin-orbit interaction in atomic physics depends also on the expectation value of $\xi(r)$. For example,

$$\begin{aligned} \langle n, j, \ell, s, m_j | \mathcal{H}'_{\text{SO}} | n, j, \ell, s, m_j \rangle &= \langle j, \ell, s, m_j | \mathbf{L} \cdot \mathbf{S} | j, \ell, s, m_j \rangle \\ &\times \int_0^\infty R_{n\ell}^* \xi(r) R_{n\ell} dr, \end{aligned} \quad (14.9)$$

where $R_{n\ell}$ (the radial part of the wave function) has an r dependence. The magnitude of the integral in (14.9) increases rapidly with increasing atomic number Z , approximately as Z^3 or Z^4 . The physical reason behind the strong Z dependence of $\langle \mathcal{H}'_{\text{SO}} \rangle$ is that atoms with high Z have more electrons to generate larger internal H fields and more electrons with magnetic moments to experience the interaction with these magnetic fields.

For most atomic species that are important in semiconducting materials, the spin-orbit interaction plays a significant role. Some typical values for the spin-orbit splitting energies ΔE for common cubic semiconductors are shown in Table 14.1, where the ΔE listing gives the Γ -point valence band splittings. We will see that in crystalline solids the spin-orbit splittings are \mathbf{k} -dependent. For example, at the L -point for cubic materials, the spin-orbit splittings are typically about 2/3 of the Γ -point value.

The one-electron Hamiltonian for a solid including spin-orbit interaction is

$$\mathcal{H} = \underbrace{\frac{p^2}{2m} + V(\mathbf{r})}_{\mathcal{H}_0} + \underbrace{\frac{1}{2m^2 c^2} (\nabla V \times \mathbf{p}) \cdot \mathbf{S}}_{\mathcal{H}'_{\text{SO}}}. \quad (14.10)$$

When the spin-orbit interaction is included, the wave functions consist of a spatial part and a spin part. This means that the irreducible representations that classify the states in a solid must depend on the spin angular momentum. To show the effect of the \mathbf{k} -dependence of the spin-orbit interaction on the energy bands of a semiconductor, consider the energy bands for germanium shown in Fig. 14.1(a) along the $\Delta(100)$ axis, $\Lambda(111)$ axis and $\Sigma(110)$ axes

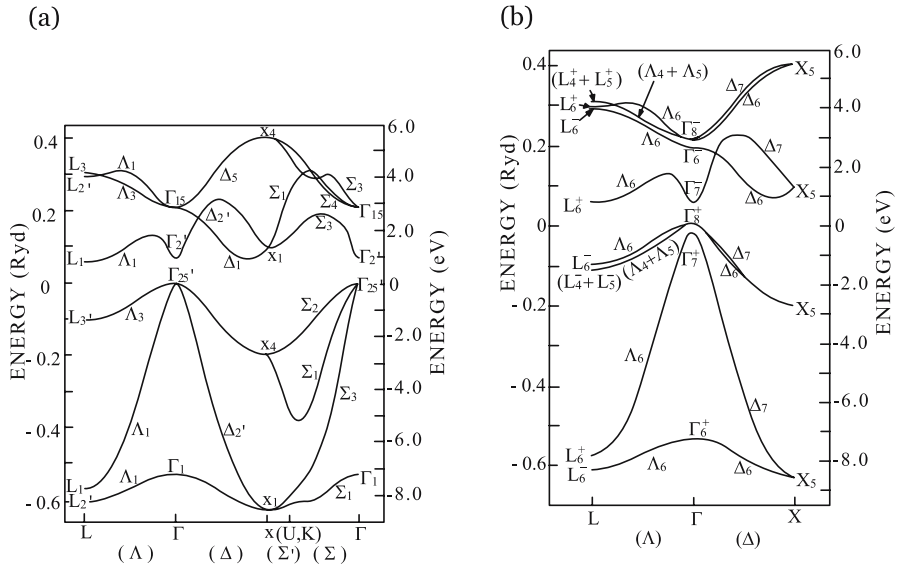


Fig. 14.1. Energy versus dimensionless wave vector for a few high-symmetry directions in germanium using standard notation. (a) The spin–orbit interaction has been neglected. (b) The spin–orbit interaction has been included and the bands are labeled by the double group representations

for no spin–orbit interaction. Here we show the four bonding and the four antibonding s - and p -bands. This picture is to be compared with the energy bands for Ge including the spin–orbit interaction shown in Fig. 14.1(b). The treatment of spin–orbit interaction in crystals that lack inversion symmetry (e.g., such as III–V compounds which have T_d symmetry) gives rise to the “Dresselhaus spin–orbit” term [25] which is often referred to in the spintronics literature. This topic is further discussed in Chap. 16 in connection with time reversal symmetry.

We note that the Fermi level is between the top of the highest valence band (the $\Gamma_{25'}$ band) and the bottom of the lowest conduction band (the L_1 band). The energy band extrema for the more common semiconductors usually occur at high symmetry points. The inclusion of the spin–orbit interaction has two major effects on the energy band structure affecting both the level degeneracies and the labeling of the energy bands. Note that the $(L_4^\pm + L_5^\pm)$ and $(\Lambda_4 + \Lambda_5)$ are Kramers-degenerate doublet states, which means that these bands stick together at high symmetry points and along high symmetry directions, because of time reversal symmetry to be discussed in Chap. 16. The Γ_7^+ band which lies below the Γ_8^+ valence band in Fig. 14.1(b) is called the *split-off band*, and the separation between the Γ_7^+ and the Γ_8^+ bands is the Γ -point spin–orbit splitting energy ΔE given in Table 14.1 for Ge.

14.2 Crystal Double Groups

Figure 14.1(b) shows energy bands that are labeled by the irreducible representations of the *double group* for the diamond structure. Double groups come into play when we are dealing with the electron spin, whereby half-integral angular momentum states are introduced. In this section we discuss the double group irreducible representations which arise when the electron spin is introduced.

The character tables for states of half-integral angular momentum are constructed from the same basic formula as we used in Chap. 5 for finding the characters for a rotation by an angle α in the full rotation group:

$$\chi_j(\alpha) = \frac{\sin(j + 1/2)\alpha}{\sin(\alpha/2)}. \quad (14.11)$$

Not only is (14.11) valid for integral j (as we have discussed in Chap. 5) but the formula is also valid for j equal to half-integral angular momentum states. We will now discuss the special issues that must be considered for the case of half-integral spin.

Firstly we note that (14.11) behaves differently under the transformation $\alpha \rightarrow (\alpha + 2\pi)$ depending on whether j is an integral or half-integral angular momentum state. This difference in behavior is responsible for the name of *double groups* when j is allowed to assume half-integral values. Let us consider how rotation by $\alpha + 2\pi$ is related to a rotation by α :

$$\chi_j(\alpha + 2\pi) = \frac{\sin(j + 1/2)(\alpha + 2\pi)}{\sin\left(\frac{\alpha + 2\pi}{2}\right)} = \frac{\sin(j + 1/2)\alpha \cdot \cos(j + 1/2)2\pi}{\sin(\alpha/2) \cdot \cos \pi}, \quad (14.12)$$

since $\sin(j + 1/2)2\pi = 0$ whether j is an integer or a half-integer. For integral values of j , $\cos(j + 1/2)2\pi = -1$ while for half-integral values of j , $\cos(j + 1/2)2\pi = +1$. Therefore we have the important relation

$$\chi_j(\alpha + 2\pi) = \chi_j(\alpha)(-1)^{2j}, \quad (14.13)$$

which implies that for integral j , a rotation by $\alpha, \alpha \pm 2\pi, \alpha \pm 4\pi$, etc. yields identical characters (integral values of j correspond to odd-dimensional representations of the full rotation group), the dimensionality being given by $2j + 1$. For half-integral values of j , corresponding to the even-dimensional representations of the rotation group, we have

$$\begin{aligned} \chi_j(\alpha \pm 2\pi) &= -\chi_j(\alpha) \\ \chi_j(\alpha \pm 4\pi) &= +\chi_j(\alpha), \end{aligned} \quad (14.14)$$

so that rotation by 4π is needed to yield the same character for $\chi_j(\alpha)$. The need to rotate by 4π (rather than by 2π) to generate the identity operation leads to the concept of double groups which is the main theme of this chapter.

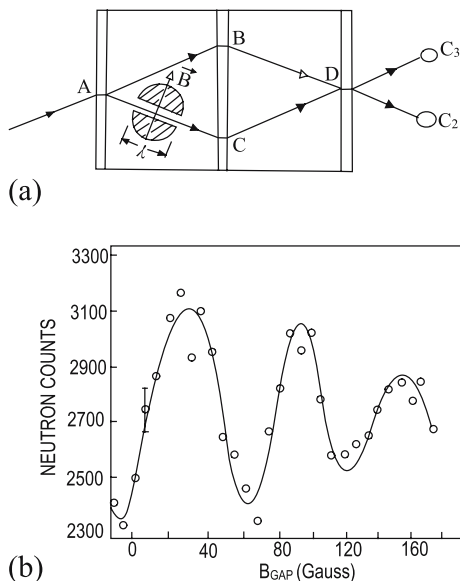


Fig. 14.2. (a) A schematic diagram of the neutron interferometer used to establish the phase of the electron wave function along the path AC along which the neutrons are in a magnetic field B (500 G) for a distance ℓ (2 cm), while the path AB has no magnetic field [72]. (b) The periodic interference pattern as a function of magnetic field, implying a periodicity of 4π

Although the concept of double groups goes back to 1929 [11] experimental evidence that wave functions for Fermions are periodic in 4π and not 2π was not available until 1975 [72] when an ingenious experiment was carried out to measure the phase shift of a neutron due to its precession in a magnetic field. The experiment utilizes a neutron interferometer and determines the phase shift of the neutron as it travels along path AC, where it sees a magnetic field B_{gap} as opposed to path AB where there is no magnetic field, as shown in Fig. 14.2(a). The phase shift measured by counters C_2 and C_3 shows an interference pattern that is periodic, as shown in Fig. 14.2(b), implying a magnetic field precession with a periodicity of 4π . To account for this behavior of the wave function, it is convenient to *introduce a new group element* (rotation by 2π) in dealing with symmetry properties of crystals for which half-integral values of the angular momentum arise as, for example, through the introduction of the electron spin.

Let \mathcal{R} denote a rotation by 2π , and now let us assume that $\mathcal{R} = \pm E$ or equivalently $\mathcal{R}^2 = E$, since the rotation by 4π leaves the characters for the full rotation group invariant for both integral and half-integral j values. Suppose that the elements of the symmetry group without the electron spin are E, A_2, A_3, \dots, A_h . Then, with spin, we have twice as many group elements. That is, we now have the same h elements of the type A_i that we had before

the spin on the electron was considered, plus h new elements of the form $\mathcal{R}A_i$. Just as the matrix representation for the identity operator E is the unit matrix $\hat{1}$ and for $\mathcal{R}E$ it is $\pm\hat{1}$, the matrix representation for A_i is $D^{(T_j)}(A_i)$ and for $\mathcal{R}A_i$ it is $\pm D^{(T_j)}(A_i)$, depending upon whether the representation T_j is related by compatibility relations to even- or odd-dimensional representations of the full rotation group. The introduction of this symmetry element \mathcal{R} leads to no difficulties with the quantum mechanical description of the problem, since the wave functions ψ and $-\psi$ describe the same physical problem and the matrices $\pm D^{(T_j)}(A_i)$ each produce the same linear combination of the basis functions.

Because of the introduction of the symmetry element \mathcal{R} , the point groups of the crystal have twice as many elements as before. These point groups also have more classes, but not exactly twice as many classes because some of the elements $\mathcal{R}A_i$ are in the same classes as other elements A_k . For example, according to (14.11), when j assumes *half-integral values*, then we have for a C_2 operation

$$\chi_j(\pi) = \frac{\sin(j + 1/2)\pi}{\sin(\pi/2)} = 0 \quad (14.15)$$

and

$$\chi_j(\pi \pm 2\pi) = \frac{\sin(j + 1/2)(\pi \pm 2\pi)}{\sin(\frac{\pi \pm 2\pi}{2})} = \frac{0}{-1} = 0. \quad (14.16)$$

As presented in Sect. 14.3, for some classes of twofold axes, the elements $\mathcal{R}C_2$ and C_2 are, in fact, in the same class.

14.3 Double Group Properties

We will now state some properties of the even-dimensional representations of the full rotation group and of double groups corresponding to the half-integral angular momentum states. These properties are given here without proof. More complete treatments can be found, for example, in Heine's book on group theory [37]. We list below four important rules for the properties of double groups.

- (a) If a set of symmetry operations $\{A_k\}$ forms a class in the original point group, then $\{A_k\}$ and the corresponding symmetry operations for the double group $\{\mathcal{R}A_k\}$ form two different classes in the double group, except in the case noted below under heading (b).
- (b) The exceptions to property (a) are classes of rotations by π , if, and only if, there is in addition to the operation C_2 another twofold axis \perp to the twofold axis C_2 for all members of the class. In this case only, C_2 and $\mathcal{R}C_2$ are in the same class.
- (c) Any irreducible representation of the original group is also an irreducible representation of the double group, with the same set of characters $[\chi(\mathcal{R}C_k) = \chi(C_k)]$.

(d) In addition to the irreducible representations described in property (c), there must be additional double group representations, so that we have as many irreducible representations as there are classes. For these additional irreducible representations, the characters for the class $\mathcal{R}C_k$ are found from the characters of class C_k according to the relation $\chi(\mathcal{R}C_k) = -\chi(C_k)$. The relation $\chi(C_k) = -\chi(\mathcal{R}C_k)$ follows because the signs of the wavefunctions change as a result of the symmetry operation $\mathcal{R}C_k$. In the special case where property (b) applies and $\{A_k\}$ and $\{\mathcal{R}A_k\}$ are in the same class, then

$$\chi(C_k) = +\chi(\mathcal{R}C_k) = -\chi(\mathcal{R}C_k) = 0, \quad (14.17)$$

since both types of symmetry operations are in same class. Therefore, for classes obeying property (b), it is always the case that $C_k = C_2$ where $\chi(C_2) = 0$.

We can now write down the characters for double group representations and relate these results to the spin–orbit interaction. In a solid, without spin–orbit coupling

$$\mathcal{H}_0 = \frac{p^2}{2m} + V(\mathbf{r}). \quad (14.18)$$

Now if we include the electron spin, but still neglect the spin–orbit interaction, the Bloch functions in the simplest case can be written as

$$\begin{aligned} \psi_{nk}^+ &= e^{i\mathbf{k}\cdot\mathbf{r}} u_{nk}(\mathbf{r})\alpha \\ \psi_{nk}^- &= e^{i\mathbf{k}\cdot\mathbf{r}} u_{nk}(\mathbf{r})\beta, \end{aligned} \quad (14.19)$$

where α, β are the spin up and spin down eigenfunctions for spin 1/2, and n, k denote the band index and wave number, respectively, and for a single electron with $S_z = \pm 1/2$. Without spin–orbit coupling, each state is doubly degenerate and is an eigenstate of S_z . If the spin–orbit interaction is included, then the states are no longer eigenstates of S_z and the wave function becomes some linear combination of the states given by (14.19)

$$\psi_{nk} = a\psi_{nk}^+ + b\psi_{nk}^-. \quad (14.20)$$

The group theoretical way to describe these states is in terms of the direct product $\Gamma_i \otimes D_{1/2}$ of the irreducible representation of the spatial wave functions Γ_i with the irreducible representation of the spin function of an electron which we will denote by $D_{1/2}$ and is called the Spinor.

To illustrate how we write the characters for $D_{1/2}$, let us consider cubic crystals with an O symmetry point group. (The results for O_h are immediately obtained from O by taking the direct product $O_h = O \otimes i$.) From the rules given above, the classes of the double group for O are $E, \mathcal{R}, (3C_4^2 +$

Table 14.2. Character for rotations by α for the full rotational symmetry group and the $j = 1/2$ Spinor irreducible representation $D_{1/2}$

| α | $\chi_{\frac{1}{2}}(\alpha)$ | $\chi_{\frac{1}{2}}(\mathcal{R}\alpha)$ |
|-----------------|--|---|
| 0 | $\frac{\alpha}{\alpha/2} = 2$ | -2 |
| π | 0 | 0 |
| $\frac{\pi}{2}$ | $\frac{\sin \frac{\pi}{2}}{\sin \frac{\pi}{4}} = \frac{1}{\frac{1}{\sqrt{2}}} = \sqrt{2}$ | $-\sqrt{2}$ |
| $\frac{\pi}{3}$ | $\frac{\sin \frac{2\pi}{3}}{\sin \frac{\pi}{3}} = \frac{\frac{\sqrt{3}}{2}}{\frac{\sqrt{3}}{2}} = 1$ | -1 |

$3\mathcal{RC}_4^2, 6C_4, 6\mathcal{RC}_4, (6C_2 + 6\mathcal{RC}_2), 8C_3, 8\mathcal{RC}_3$. Having listed the classes (eight in this case), we can now find the characters for $D_{1/2}$ by the formula

$$\chi_j(\alpha) = \frac{\sin(j + 1/2)\alpha}{\sin(\alpha/2)} = \frac{\sin \alpha}{\sin(\alpha/2)}, \tag{14.21}$$

since $j = 1/2$. For the Full Rotational Symmetry group, the characters for a rotation by α for the double point group O are found using (14.21) and the results are given in Table 14.2. This procedure for finding the characters for the spinor $D_{1/2}$ is general and can be done for any point group.

Now we will write down the complete character table for the double group O . In O itself, there are 24 elements, and therefore in the double group derived from O there are $24 \times 2 = 48$ elements. There are eight classes in the double group O and therefore eight irreducible representations. We already have five of these irreducible representations (see Table 14.3 for group O). These five irreducible representations are all even representations of the group O_h (see Table D.1 for the corresponding basis functions). Using rule (b) in Sect. 14.3 for the character tables of double group representations, we have the following condition for the dimensionality of the three additional double group representations ($\Gamma_6, \Gamma_7, \Gamma_8$) that are not present in the original group O

$$\sum_i \ell_i^2 = h \tag{14.22}$$

$$1^2 + 1^2 + 2^2 + 3^2 + 3^2 + \ell_6^2 + \ell_7^2 + \ell_8^2 = 48, \tag{14.23}$$

yielding the following restriction on the dimensionalities of the double group irreducible representations:

$$\ell_6^2 + \ell_7^2 + \ell_8^2 = 24. \tag{14.24}$$

Table 14.3. Worksheet for the double group characters for the group O

| | E | \mathcal{R} | $3C_4^2 + 3\mathcal{R}C_4^2$ | $6C_4$ | $6\mathcal{R}C_4$ | $6C_2' + 6\mathcal{R}C_2''$ | $8C_3$ | $8\mathcal{R}C_3$ |
|----------------|-----|---------------|------------------------------|------------|-------------------|-----------------------------|--------|-------------------|
| Γ_1 | 1 | 1 | 1 | 1 | 1 | 1 | 1 | 1 |
| Γ_2 | 1 | 1 | 1 | -1 | -1 | -1 | 1 | 1 |
| Γ_{12} | 2 | 2 | 2 | 0 | 0 | 0 | -1 | -1 |
| $\Gamma_{15'}$ | 3 | 3 | -1 | 1 | 1 | -1 | 0 | 0 |
| $\Gamma_{25'}$ | 3 | 3 | -1 | -1 | -1 | 1 | 0 | 0 |
| Γ_6 | 2 | -2 | 0 | $\sqrt{2}$ | $-\sqrt{2}$ | 0 | 1 | -1 |
| Γ_7 | 2 | -2 | 0 | | | 0 | | |
| Γ_8 | 4 | -4 | 0 | | | 0 | | |

Table 14.4. Characters used to find entries x and y for representation Γ_7

| | E | $8C_3$ | $6C_4$ |
|------------|-----|--------|------------|
| Γ_6 | 2 | 1 | $\sqrt{2}$ |
| Γ_7 | 2 | x | y |

Table 14.5. Characters used to find entries x' and y' for representation Γ_8

| | E | $8C_3$ | $6C_4$ |
|------------|-----|--------|-------------|
| Γ_6 | 2 | 1 | $\sqrt{2}$ |
| Γ_7 | 2 | 1 | $-\sqrt{2}$ |
| Γ_8 | 4 | x' | y' |

This allows us to fill in many of the entries in the double group character table for group O (Table 14.3). For example, Γ_6 , Γ_7 and Γ_8 cannot have 5-dimensional representations, because then $\ell_j^2 = 25 > 24$. Among 1-, 2-, 3- and 4-dimensional irreducible representations, the only combination we can make to satisfy (14.24) is

$$2^2 + 2^2 + 4^2 = 24. \tag{14.25}$$

We already have identified a 2-dimensional irreducible representation of the double group, namely the “spinor” $D_{1/2}$ (see Table 14.2). We see immediately that $D_{1/2}$ obeys all the orthogonality relations, and the characters for $D_{1/2}$ can be added to the character table, using the notation $D_{1/2} = \Gamma_6$.

In Table 14.3 we have also filled in zeros for the characters for all the C_2 classes in the special double group representations Γ_6 , Γ_7 and Γ_8 . Using orthogonality and normalization conditions which follow from the wonderful orthogonality theorem on character, it is quite easy to complete this character table. To get the Γ_7 representation we have to consider the entries in Table 14.4 and orthogonality requires $4 + 8x + 6\sqrt{2}y = 0$ which is satisfied for $x = \pm 1$, and $y = -\sqrt{2}$. Having filled in those entries it is easy to get the four-dimensional representation (see Table 14.5). Orthogonality now requires: $8 + 8x' \pm \sqrt{2}y' = 0$

Table 14.6. Double group character table for the group O

| O | E | \mathcal{R} | $3C_4^2 + 3\mathcal{R}C_4^2$ | $6C_4$ | $6\mathcal{R}C_4$ | $6C_2' + 6\mathcal{R}C_2''$ | $8C_3$ | $8\mathcal{R}C_3$ |
|----------------|-----|---------------|------------------------------|-------------|-------------------|-----------------------------|--------|-------------------|
| Γ_1 | 1 | 1 | 1 | 1 | 1 | 1 | 1 | 1 |
| Γ_2 | 1 | 1 | 1 | -1 | -1 | -1 | 1 | 1 |
| Γ_{12} | 2 | 2 | 2 | 0 | 0 | 0 | -1 | -1 |
| $\Gamma_{15'}$ | 3 | 3 | -1 | 1 | 1 | -1 | 0 | 0 |
| $\Gamma_{25'}$ | 3 | 3 | -1 | -1 | -1 | 1 | 0 | 0 |
| Γ_6 | 2 | -2 | 0 | $\sqrt{2}$ | $-\sqrt{2}$ | 0 | 1 | -1 |
| Γ_7 | 2 | -2 | 0 | $-\sqrt{2}$ | $\sqrt{2}$ | 0 | 1 | -1 |
| Γ_8 | 4 | -4 | 0 | 0 | 0 | 0 | -1 | 1 |

Table 14.7. Direct products $\Gamma_i \otimes \Gamma_6^+$ for O_h symmetry

| | |
|---|---|
| $\Gamma_1^+ \otimes \Gamma_6^+ = \Gamma_6^+$ | $\Gamma_1^- \otimes \Gamma_6^+ = \Gamma_6^-$ |
| $\Gamma_2^+ \otimes \Gamma_6^+ = \Gamma_7^+$ | $\Gamma_2^- \otimes \Gamma_6^+ = \Gamma_7^-$ |
| $\Gamma_{12}^+ \otimes \Gamma_6^+ = \Gamma_8^+$ | $\Gamma_{12}^- \otimes \Gamma_6^+ = \Gamma_8^-$ |
| $\Gamma_{15}^+ \otimes \Gamma_6^+ = \Gamma_6^+ + \Gamma_8^+$ | $\Gamma_{15}^- \otimes \Gamma_6^+ = \Gamma_6^- + \Gamma_8^-$ |
| $\Gamma_{25}^+ \otimes \Gamma_6^+ = \Gamma_7^+ + \Gamma_8^+$ | $\Gamma_{25}^- \otimes \Gamma_6^+ = \Gamma_7^- + \Gamma_8^-$ |
| $\Gamma_6^+ \otimes \Gamma_6^+ = \Gamma_1^+ + \Gamma_{15}^+$ | $\Gamma_6^- \otimes \Gamma_6^+ = \Gamma_1^- + \Gamma_{15}^-$ |
| $\Gamma_7^+ \otimes \Gamma_6^+ = \Gamma_2^+ + \Gamma_{25}^+$ | $\Gamma_7^- \otimes \Gamma_6^+ = \Gamma_2^- + \Gamma_{25}^-$ |
| $\Gamma_8^+ \otimes \Gamma_6^+ = \Gamma_{12}^+ + \Gamma_{15}^+ + \Gamma_{25}^+$ | $\Gamma_8^- \otimes \Gamma_6^+ = \Gamma_{12}^- + \Gamma_{15}^- + \Gamma_{25}^-$ |

which is satisfied for $x' = -1$, $y' = 0$. So now we have the whole character table, as shown in Table 14.6.

In practice, we do not have to construct these character tables because the double group character tables have already been tabulated in the literature [47, 48, 54] or via the website cited in Ref. [54]. An example of a double group character table for O symmetry is given in Appendix D, Table D.1. Here you will see that a symmetry element RC_n is listed as \overline{R}_n following the notation in Koster's book. Other examples of double group character tables are found in Appendix D.

We will now apply the double group characters to a cubic crystal with O_h symmetry at the Γ point, $\mathbf{k} = 0$ and we make use of Table 14.6 or Table D.1 and $O_h = O \otimes i$ or Table D.1. The spin functions α and β transform as the partners of the irreducible representation $D_{1/2}$ which is written as Γ_6^+ for the double group O_h . Now we see that the appropriate double group representations (which must be used when the effects of the electron spin are included) are obtained by taking the direct product of the irreducible representation Γ_i with the spinor ($D_{1/2}$) as shown in Table 14.7. Since group $O_h = O \otimes i$, the number of classes in the double group O_h is $2 \times 8 = 16$ and the total number of irreducible representations is 16, and each is labeled according to whether

it is even or odd under the inversion operation, noting that $\Gamma'_{15} = \Gamma_{15}^+$ and $\Gamma'_{25} = \Gamma_{25}^+$, while $\Gamma_{15} = \Gamma_{15}^-$ and $\Gamma_{25} = \Gamma_{25}^-$.

When the spin–orbit interaction is introduced into the description of the electronic structure, then the energy bands are labeled by double group irreducible representations (e.g., Γ_6^\pm , Γ_7^\pm and Γ_8^\pm for the O_h group at $\mathbf{k} = 0$). Table 14.7 shows that the one-dimensional representations without the spin–orbit interaction Γ_1^\pm and Γ_2^\pm all become *doubly degenerate* after taking the direct product with the spinor $D_{1/2}$. This result is independent of the symmetry group. When the spin–orbit interaction is introduced, all formerly non-degenerate levels therefore become double degenerate as in Fig. 14.1(b). (This effect is called the *Kramers degeneracy*.)

In the case of the O_h group, the twofold levels Γ_{12}^\pm become fourfold degenerate when spin is included as is shown in Table 14.7. However, something different happens for the triply degenerate Γ_{15}^\pm and Γ_{25}^\pm states. These states would become sixfold degenerate with spin, but the spin–orbit interaction partly lifts this degeneracy so that these sixfold levels split into a twofold and a fourfold level, just as in the atomic case. Group theory does not tell us the ordering of these levels, nor the magnitude of the splitting, but it does give the symmetry of the levels. By including the spin–orbit interaction in dealing with the valence band of a semiconductor like germanium, the sixfold level can be partially diagonalized; the (6×6) $\mathbf{k} \cdot \mathbf{p}$ effective Hamiltonian breaks up into a (2×2) block and a (4×4) block.

Figure 14.1 shows the effect of the spin–orbit interaction on the energy bands of germanium. We note that the magnitudes of the spin–orbit splittings are *\mathbf{k} dependent*. Spin–orbit effects are largest at $\mathbf{k} = 0$, moderately large along the (111) direction (A) and at the L -point, but much smaller along the (100) direction (Δ) and at the X -point. Group theory does not provide information on these relative magnitudes. As was mentioned above, the spin–orbit interaction effects tend to be very *important* in the **III–V compound semiconductors**. Since in this case the two atoms in the unit cell correspond to different chemical species, the appropriate point group at $\mathbf{k} = 0$ is T_d and the bonding and antibonding bands both have symmetries Γ_1 and Γ_{15} for the s and p states, respectively. The general picture of the energy bands for the III–V compounds is qualitatively similar to that given in Fig. 14.1 except for a generally larger spin–orbit splitting and for a linear k term to be discussed with regard to time reversal symmetry (see Chap. 16).

Another important class of semiconductors where the spin–orbit interaction is important is the narrow gap lead salts (e.g., PbTe). Since Pb has a high atomic number, it is necessary to give a more exact theory for the spin–orbit interaction in this case, by including relativistic correction terms [21]. However, the group theoretical considerations given here apply equally well when relativistic corrections are included.

In writing down the double group irreducible representations, we see that a particular representation may be associated with various single group representations. For example, the direct products in Table 14.7 show that the

Γ_7^+ irreducible double group representation could be associated with either a Γ_2^+ or a Γ_{25}^+ irreducible single group representation. In dealing with basis functions in the double group representations, it is often useful to know which single group representation corresponds to a particular double group representation. The standard notation used for this association is for example $\Gamma_8^+(\Gamma_{12}^+)$, in which the appropriate single group representation is put in parenthesis, indicating that the particular Γ_8^+ basis functions of interest are those arising from the direct product $\Gamma_{12}^+ \otimes \Gamma_6^+$ rather than from one of the other possibilities listed in Table 14.7.

14.4 Crystal Field Splitting Including Spin–Orbit Coupling

In our treatment of crystal field splittings in solids in Chap. 5 we ignored the spin–orbit coupling, thus providing a first approximation for describing the crystal field levels for the impurity ions in a host lattice. To improve on this, we consider in this chapter the effect of the spin–orbit interaction which will allow us to treat crystal field splittings in host lattices with rare earth ions (where the spin–orbit interaction is in fact larger than the crystal field interaction), and also to obtain a better approximation to the crystal field splittings for $3d$ transition metal ions that were first discussed in Chap. 5.

The introduction of a transition-metal ion in an atomic d -state into an octahedral crystal field gives rise to crystal field splittings, as shown in Fig. 14.3 (see also Sect. 5.3).

For a single d -electron, $s = 1/2$ and in O_h symmetry the appropriate double group representation for the spinor is Γ_6^+ . Thus when the spin–orbit interaction is included in the crystal field problem, the d -levels are further split. Thus the twofold crystal field level in O_h cubic symmetry transforms as

$$\Gamma_{12}^+ \otimes \Gamma_6^+ = \Gamma_8^+ \quad (14.26)$$

and the threefold crystal field level in O_h symmetry is split according to

$$\Gamma_{25}^+ \otimes \Gamma_6^+ = \Gamma_7^+ + \Gamma_8^+ . \quad (14.27)$$

In (14.26) and (14.27), Γ_{12}^+ and Γ_{25}^+ denote spatial wave-functions and Γ_6^+ denotes the spin wave-function. Here we see that the E_g (Γ_{12}^+) level does not split further by the spin-orbit interaction, but the T_{2g} (Γ_{25}^+) level splits into a twofold and a fourfold level.

For the 2D state of the free $3d$ transition-metal ion, we use to Fig. 14.3 to show the splitting induced by a large crystal field and a small spin-orbit interaction (where the number of states is given in parentheses and we use the notation ${}^{2s+1}X_J$ to denote the quantum numbers s and J while X denotes the orbital angular momentum). The analysis in Fig. 14.3 is valid only if the *crystal field interaction is large compared with the spin-orbit splitting*. This situation describes the iron-group transition metal ions.

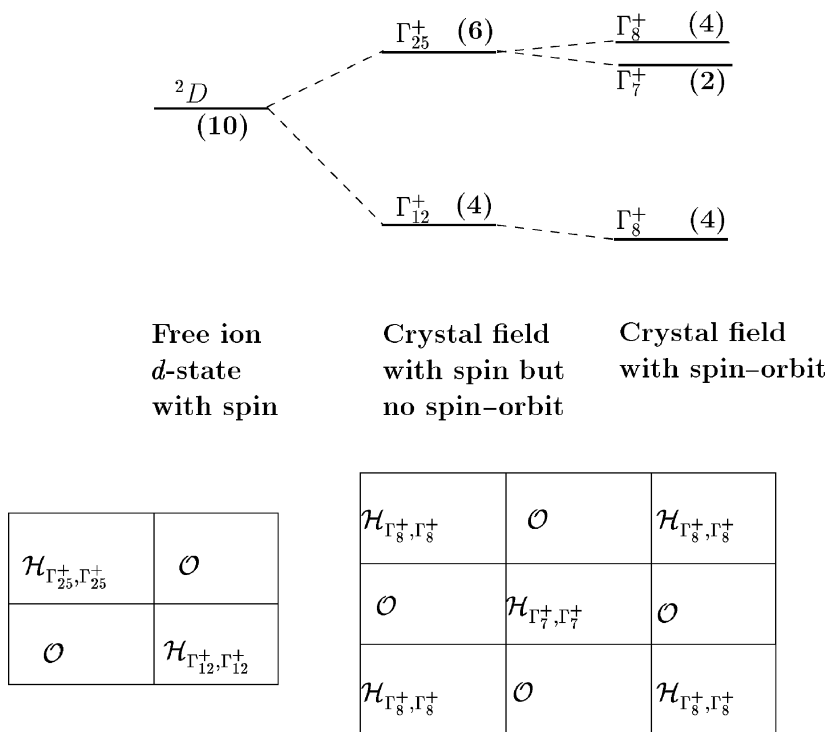
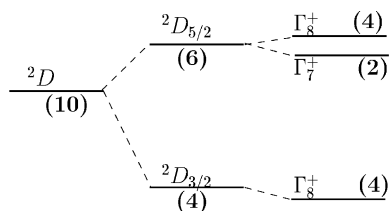


Fig. 14.3. Schematic diagram of the crystal field splitting of a 2D state with a tenfold degeneracy, followed by further splitting by the spin–orbit interaction. This model is appropriate for a $3d$ transition metal ion in a crystal with O_h symmetry for which the crystal field perturbation is large compared to the spin–orbit interaction. The degeneracy of each of the levels is indicated by the parentheses. Also shown in this figure are the labels for the crystal field levels associated with each of the Γ_8^+ levels in the absence of the spin–orbit interaction. Below the crystal field splitting diagram, the form of the crystal field Hamiltonian is indicated on the left in the absence of the spin–orbit interaction, and on the right when the spin–orbit interaction is included

When we move down the periodic table to the palladium group ($4d$) and the platinum group ($5d$), the spin–orbit interaction becomes large compared with the crystal field. In this case, we consider first the spin–orbit splitting of the free ion state as the major perturbation (see Fig. 14.4). We now have to consider the effect of the crystal field on levels described by half-integral j values. To compute the characters for the full rotation group, we use the formula

$$\chi_j(\alpha) = \frac{\sin(j + 1/2)\alpha}{\sin(\alpha/2)}. \tag{14.28}$$

We then find the characters for the ${}^2D_{5/2}$ and ${}^2D_{3/2}$ states to see how they split in the cubic field (see Table 14.8). Using Table 14.8 we see immediately



| | |
|-----------------|----------------------------|
| Free ion | Crystal field |
| <i>d</i> -state | Spin-orbit with spin-orbit |
| with spin | |

Fig. 14.4. Schematic diagram of the spin–orbit splitting of a 2D level with a tenfold degeneracy and of the subsequent crystal field splittings of these levels in a cubic field for an ion with a spin–orbit interaction that is large compared to the crystal field splittings (which might apply to a $4d$ or a $5d$ atomic level). The degeneracy of each level is shown in parentheses

that the irreducible representations for ${}^2D_{5/2}$ and ${}^2D_{3/2}$ become

$${}^2D_{5/2} \rightarrow \Gamma_7 + \Gamma_8 \quad (14.29)$$

$${}^2D_{3/2} \rightarrow \Gamma_8 \quad (14.30)$$

as indicated in Fig. 14.4. The symmetries in Figs. 14.3 and 14.4 for the levels in the presence of both the spin–orbit interaction and the cubic field of the crystalline solid are $\Gamma_7^+ + 2\Gamma_8^+$ in both cases with the + parity coming from the orbital angular momentum being a D -level (even parity state). In Fig. 14.4, the crystal field splittings are small compared with the spin–orbit splittings, in contrast to the case in Fig. 14.3.

Let us consider another example of crystal field levels that show some other important features. Consider the levels of the holmium ion Ho^{3+} in a cubic field (group O) for which the atomic configuration is $4f^{10}5s^25p^6$ so that by Hund’s rule the ground state, after the spin–orbit interaction is included, becomes, $s = 2$, $l = 6$, $j = 8$ denoted by the spectroscopic notation 5I_8 (see page 404 of Ref. [45]). Since $j = 8$ is an integer, application of the formula

$$\chi_j(\alpha) = \left\{ \frac{\sin(j + 1/2)\alpha}{\sin(\alpha/2)} \right\} \quad (14.31)$$

gives only ordinary irreducible representations, even though the electron spin is included. We thus get the characters for the ground state 5I_8 given in Table 14.9.

Decomposition of the $\Gamma({}^5I_8)$ level into irreducible representations of O yields

$$\Gamma({}^5I_8) \rightarrow \Gamma_1 + 2\Gamma_{12} + 2\Gamma_{15} + 2\Gamma_{25}, \quad (14.32)$$

Table 14.8. Decomposition into double group O_h representations for a $\ell = 2$ level

| | E | \mathcal{R} | $3C_4^2 + 3\mathcal{R}C_4^2$ | $6C_4$ | $6\mathcal{R}C_4$ | $6C_2 + 6\mathcal{R}C_2$ | $8C_3$ | $8\mathcal{R}C_3$ |
|-------------------|-----|---------------|------------------------------|-------------|-------------------|--------------------------|--------|-------------------|
| $\chi(^2D_{5/2})$ | 6 | -6 | 0 | $-\sqrt{2}$ | $\sqrt{2}$ | 0 | 0 | 0 |
| $\chi(^2D_{3/2})$ | 4 | -4 | 0 | 0 | 0 | 0 | -1 | 1 |

Table 14.9. Characters for the 5I_8 and $^4I_{15/2}$ states in O symmetry

| | E | $3C_4^2$ | $6C_4$ | $6C_2$ | $8C_3$ |
|----------------------|-----|----------|--------|--------|--------|
| $\Gamma(^5I_8)$ | 17 | 1 | 1 | 1 | -1 |
| $\Gamma(^4I_{15/2})$ | 16 | 0 | 0 | 0 | -1 |

where there are seven levels for 17 states. Finding the crystal field splittings for a 17-fold level would be a very difficult problem without group theory. As another example, let us consider the erbium ion Er^{3+} in a host crystal. This ion is the basis for applications of amplification capabilities in optical fibers. We consider the level splitting for the rare earth ion Er^{3+} in a $4f^{11}5s^2p^6$ which gives a $^4I_{15/2}$ ground state. The characters for the $j = 15/2$ state are given in Table 14.9 and the splitting of these states in a cubic O field is also included in this table. The $j = 15/2$ state in cubic O symmetry splits into

$$\Gamma(^4I_{15/2}) \rightarrow \Gamma_6 + \Gamma_7 + 3\Gamma_8.$$

In dealing with the crystal field problem, we often encounter a situation where a perturbation is applied to lower the crystal symmetry. In such cases we follow the procedure which we have used many times before – the irreducible representation of the high symmetry group is treated as a reducible representation for the lower symmetry group and we look for the irreducible representations contained therein. The only difference in including the spin–orbit interaction is the use of double groups for all point groups – both for the high symmetry and the low symmetry groups. It is the case that the single group irreducible representations in a group of higher symmetry will always go into single group irreducible representations of the lower symmetry group. For example, the level Γ_8 in point group O goes into $\Gamma_4 + \Gamma_5 + \Gamma_6$ in point group D_3 , when the symmetry is lowered (see Table D.7 in Appendix D.)

In considering optical transitions in semiconductors which are described by either single or double group representations, the electromagnetic interaction Hamiltonian will in all cases transform as the vector within the single group representations. Suppose that we consider the application of an electromagnetic light wave on a Ge crystal where we are considering the coupling of light to the Γ_7^- conduction band at the center of the Brillouin zone. Then we can write

$$\Gamma_{15}^- \otimes \Gamma_7^- = \Gamma_7^+ + \Gamma_8^+, \quad (14.33)$$

and see that light couples the conduction band at $k = 0$ to the valence band and to its related split-off band. Thus, if single group states had been considered instead, such as the Γ_2^- conduction band in Ge without spin-orbit interaction, the coupling of the Γ_2^- band by light would be found by ($\Gamma_{15}^- \otimes \Gamma_2^- = \Gamma_{25}^+$), which tells us that the Γ_7^- conduction band and the Γ_{25}^+ valence band are in this case also coupled by light. Then (14.33) shows that the corresponding double group conduction band state (Γ_7^-) is optically coupled to the corresponding double group valence band states ($\Gamma_7^+ + \Gamma_8^+$).

Whereas the wave function for a single electron transforms as $D_{1/2}$ (or Γ_6^+ for O_h symmetry), a two-electron wavefunction transforms as the direct product $D_{1/2} \otimes D_{1/2}$. For O_h symmetry, we have for this direct product

$$\Gamma_6^+ \otimes \Gamma_6^+ = \Gamma_1^+ + \Gamma_{15}^+, \quad (14.34)$$

where Γ_1^+ is the singlet $s = 0$ state and the Γ_{15}^+ corresponds to the triplet $s = 1$ level which has three values of m_s . More explicitly, using \uparrow and \downarrow to denote the two spin states and the numerals 1 and 2 to denote each of the two electrons, we can denote the $s = 0$ state by $1/\sqrt{2}(\uparrow_1\downarrow_2 - \downarrow_1\uparrow_2)$ and the three partners of $s = 1$ by $(\uparrow_1\uparrow_2)$, $1/\sqrt{2}(\uparrow_1\downarrow_2 + \downarrow_1\uparrow_2)$, and $(\downarrow_1\downarrow_2)$. We note that in both cases, the levels have integral values of spin angular momentum and thus the state transforms as a single group irreducible representation. Finally, we note that for a $D_{3/2}$ in full rotational symmetry generated by two p -electrons, the double group representation in cubic symmetry for two p electrons yields $D_{1/2}^+ \otimes \Gamma_{15}^- = \Gamma_6^- + \Gamma_8^-$. For the Γ_8^- level, the m_j values are $3/2, 1/2, -1/2$ and $-3/2$ with very different wave functions than arise for the case of two electrons in s states. The $D_{1/2}^-$ level is made up of p states with $m_j = 1/2$ and $-1/2$ values. These topics are further considered in the following sections.

14.5 Basis Functions for Double Group Representations

We will use the following notation for single electron spin states:

$$\begin{aligned} \uparrow &= \text{spin up} = \begin{pmatrix} 1 \\ 0 \end{pmatrix} \\ \downarrow &= \text{spin down} = \begin{pmatrix} 0 \\ 1 \end{pmatrix}. \end{aligned} \quad (14.35)$$

The states in (14.35) are the states for the spinor $D_{1/2}$ irreducible representation. For the cubic group O this spinor is denoted by the double group representation Γ_6 and for the O_h group by Γ_6^+ . Operation by the *Pauli spin matrices* σ_x, σ_y and σ_z

$$\begin{aligned}
\sigma_x &= \begin{pmatrix} 0 & 1 \\ 1 & 0 \end{pmatrix} \\
\sigma_y &= \begin{pmatrix} 0 & -i \\ i & 0 \end{pmatrix} \\
\sigma_z &= \begin{pmatrix} 1 & 0 \\ 0 & -1 \end{pmatrix}
\end{aligned} \tag{14.36}$$

on the pure spin up and spin down states yields

$$\begin{aligned}
\sigma_x \uparrow &= \downarrow \\
-i\sigma_y \uparrow &= \downarrow \\
\sigma_z \uparrow &= \uparrow \\
\sigma_x \downarrow &= \uparrow \\
-i\sigma_y \downarrow &= -\uparrow \\
\sigma_z \downarrow &= -\downarrow .
\end{aligned} \tag{14.37}$$

The Pauli spin matrices $\sigma_x, \sigma_y, \sigma_z$ together with the (2×2) unit matrix

$$\hat{1} = \begin{pmatrix} 1 & 0 \\ 0 & 1 \end{pmatrix} \tag{14.38}$$

span a 2×2 space, so that every 2×2 matrix can be expressed in terms of these four matrices, $\hat{1}, \sigma_x, -i\sigma_y, \sigma_z$. Also the raising σ_+ and lowering σ_- operators are defined by

$$\sigma_{\pm} = \sigma_x \pm i\sigma_y, \tag{14.39}$$

so that

$$\frac{1}{2}\sigma_- \uparrow = \downarrow \quad \text{and} \quad \frac{1}{2}\sigma_+ \downarrow = \uparrow . \tag{14.40}$$

One set of basis functions for Γ_6^+ is the pair \uparrow, \downarrow which form partners for Γ_6^+ relevant to spinors. This pair is also referred to as $[\phi(1/2, 1/2)$ and $\phi(1/2, -1/2)]$ denoting the s and m_s values for each partner. Any other pair can be found from multiplication of this pair by another basis function such as Γ_1^+ , since $\Gamma_6^+ = \Gamma_1^+ \otimes \Gamma_6^+$. We will see below how very different-looking basis functions can be used for Γ_6^+ depending on the single group representation with which Γ_6^+ is connected, such as a Γ_1^+ or a Γ_{15}^+ state. Thus, it is convenient to label the basis functions for any double group representation with the single group representation from which it comes. Thus the pair \uparrow, \downarrow would be associated with a $\Gamma_6^+(\Gamma_1^+)$ state, whereas $\Gamma_6^+(\Gamma_{15}^+)$ would have a different significance as discussed below.

To understand this notation better, consider the $\Gamma_8^+(\Gamma_{15}^+)$ state which comes from the direct product $\Gamma_{15}^+ \otimes \Gamma_6^+ = \Gamma_6^+ + \Gamma_8^+$. For the Γ_{15}^+ state

we may select the *basis functions* L_x, L_y, L_z (angular momentum components). Then the six functions $L_x \uparrow, L_x \downarrow, L_y \uparrow, L_y \downarrow, L_z \uparrow, L_z \downarrow$ make up basis functions for the combined Γ_6^+ and Γ_8^+ representations, assuming no spin-orbit interaction. However, when the spin-orbit interaction is included, we must now find the correct linear combinations of the above six functions so that two of these transform as Γ_6^+ and four transform as Γ_8^+ . The *correct linear combinations* are found by identifying those basis functions which arise in the electronic energy band problem with by making use of angular momentum states as discussed in Sect. 14.6. The principles of group theory tell us that if the group theory problem is solved for angular momentum functions, then the same group theoretical solution can be applied to the electronic energy band eigenfunctions with the same symmetry. This approach is utilized in the following two sections.

14.6 Some Explicit Basis Functions

In this section, we will generate the basis functions for the $j = 3/2, \ell = 1, s = 1/2$ states and for the $j = 1/2, \ell = 1, s = 1/2$ states. For the angular momentum functions in the $|\ell s m_\ell m_s\rangle$ representation, the six eigenfunctions correspond to the orbital states $\ell = 1, m_\ell = 1, 0, -1$ and the spin states $s = 1/2, m_s = 1/2, -1/2$. The transformations we are looking for will transform these states into $j = 3/2, m_j = 3/2, 1/2, -1/2, -3/2$ and $j = 1/2, m_j = 1/2, -1/2$. The matrices which carry out these transformations generate what are known as the Clebsch-Gordan coefficients. Tables of Clebsch-Gordan coefficients are found in quantum mechanics and group theory books for many of the useful combinations of spin and orbital angular momentum that occur in practical problems [20].

A basis set that is appropriate for $\ell = 1, s = 1/2$ is given below for a Γ_8^+ double group state derived from a Γ_{15}^+ single group state (see also Sect. 14.9)

| $ j, m_j\rangle$ State | Basis Function | |
|-------------------------------------|---|---------|
| $ \frac{3}{2}, \frac{3}{2}\rangle$ | $\xi_1 = \frac{1}{\sqrt{2}}(L_x + iL_y) \uparrow$ | |
| $ \frac{3}{2}, \frac{1}{2}\rangle$ | $\xi_2 = \frac{1}{\sqrt{6}}[(L_x + iL_y) \downarrow + 2L_z \uparrow]$ | (14.41) |
| $ \frac{3}{2}, -\frac{1}{2}\rangle$ | $\xi_3 = \frac{1}{\sqrt{6}}[(L_x - iL_y) \uparrow + 2L_z \downarrow]$ | |
| $ \frac{3}{2}, -\frac{3}{2}\rangle$ | $\xi_4 = \frac{1}{\sqrt{2}}(L_x - iL_y) \downarrow$ | |

These basis functions are obtained using the fundamental relations for raising operators

$$\begin{aligned}
 L_+ |\ell, m_\ell\rangle &= \sqrt{(\ell - m_\ell)(\ell + m_\ell + 1)} |\ell, m_\ell + 1\rangle \\
 J_+ |j, m_j\rangle &= \sqrt{(j - m_j)(j + m_j + 1)} |j, m_j + 1\rangle.
 \end{aligned}
 \tag{14.42}$$

We further note that the state $|j = 3/2, m_j = -3/2\rangle$ is identical with the state for $\ell = 1, s = 1/2$ and $|m_\ell = -1, m_s = -1/2\rangle$. Therefore, we start with the $j = 3/2, m_j = -3/2$ state and apply the raising operator to obtain the other states:

$$\begin{aligned}
 J_+ \left| j = \frac{3}{2}, m_j = -\frac{3}{2} \right\rangle &= \sqrt{\left(\frac{3}{2} + \frac{3}{2}\right) \left(\frac{3}{2} - \frac{3}{2} + 1\right)} \left| j = \frac{3}{2}, m_j = -\frac{1}{2} \right\rangle \\
 &= (L_+ + S_+) \left| m_\ell = -1, m_s = -\frac{1}{2} \right\rangle \\
 &= \sqrt{(1+1)(1-1+1)} \left| m_\ell = 0, m_s = -\frac{1}{2} \right\rangle \quad (14.43) \\
 &\quad + \sqrt{\left(\frac{1}{2} + \frac{1}{2}\right) \left(\frac{1}{2} - \frac{1}{2} + 1\right)} \left| m_\ell = -1, m_s = \frac{1}{2} \right\rangle.
 \end{aligned}$$

Collecting terms, we obtain

$$\left| j = \frac{3}{2}, m_j = -\frac{1}{2} \right\rangle = \frac{\sqrt{2}}{3} \left| m_\ell = 0, m_s = -\frac{1}{2} \right\rangle + \frac{1}{\sqrt{3}} \left| m_\ell = -1, m_s = \frac{1}{2} \right\rangle. \quad (14.44)$$

We make the identification:

$$\begin{aligned}
 m_\ell = +1 &\rightarrow \frac{1}{\sqrt{2}}(L_x + iL_y) \\
 m_\ell = 0 &\rightarrow L_z \\
 m_\ell = -1 &\rightarrow \frac{1}{\sqrt{2}}(L_x - iL_y) \\
 m_s = \frac{1}{2} &\rightarrow \uparrow \\
 m_s = -\frac{1}{2} &\rightarrow \downarrow,
 \end{aligned}$$

from which we obtain the basis functions

| $ j, m_j\rangle$ State | Basis Function | |
|--|---|---------|
| $\left \frac{3}{2}, -\frac{3}{2}\right\rangle$ | $\frac{1}{\sqrt{2}}(L_x - iL_y) \downarrow$ | (14.45) |
| $\left \frac{3}{2}, -\frac{1}{2}\right\rangle$ | $\frac{1}{\sqrt{6}}[(L_x - iL_y) \uparrow + 2L_z \downarrow]$ | |

Similarly, operation of J_+ on the state $|j = 3/2, m_j = -1/2\rangle$ results in a state $|j = 3/2, m_j = 1/2\rangle$ and operation of $L_+ + S_+$ on the corresponding functions of $|m_\ell = 0, m_s = -1/2\rangle$ and $|m_\ell = -1, m_s = 1/2\rangle$ results in states $|m_\ell = 0, m_s = 1/2\rangle$ and $|m_\ell = +1, m_s = -1/2\rangle$. In this way we obtain all the basis functions for $\Gamma_8^+(\Gamma_{15}^+)$ given in (14.41).

We will now proceed to obtain the basis functions for $\Gamma_6^+(\Gamma_{15}^+)$ which are

| $ j, m_j\rangle$ State | Basis Function | |
|-------------------------------------|---|---------|
| $ \frac{1}{2}, \frac{1}{2}\rangle$ | $\lambda_1 = \frac{1}{\sqrt{3}}[(L_x + iL_y) \downarrow - L_z \uparrow]$ | (14.46) |
| $ \frac{1}{2}, -\frac{1}{2}\rangle$ | $\lambda_2 = \frac{1}{\sqrt{3}}[-(L_x - iL_y) \uparrow + L_z \downarrow]$ | |

The notation “ ξ_i ” was used in (14.41) to denote the four $\Gamma_8^+(\Gamma_{15}^+)$ basis functions for $j = 3/2$ and “ λ_i ” for the two $\Gamma_6^+(\Gamma_{15}^+)$ basis functions for $j = 1/2$. This notation “ ξ_i ” and “ λ_i ” is arbitrary and is not standard in the literature.

To obtain the $\Gamma_6^+(\Gamma_{15}^+)$ basis functions we note that the appropriate (m_ℓ, m_s) quantum numbers corresponding to $j = 1/2$ and $m_j = \pm 1/2$ are

$$\begin{aligned} m_\ell = 0, \quad m_s = \pm \frac{1}{2}, \\ m_\ell = 1, \quad m_s = -\frac{1}{2}, \\ m_\ell = -1, \quad m_s = +\frac{1}{2}, \end{aligned}$$

so that the corresponding basis functions are completely specified by making them orthogonal to the $|j = 3/2, m_j = +1/2\rangle$ and $|j = 3/2, m_j = -1/2\rangle$ states. For example, the function orthogonal to

$$\sqrt{\frac{2}{3}} \left| m_\ell = 0, m_s = -\frac{1}{2} \right\rangle + \frac{1}{\sqrt{3}} \left| m_\ell = -1, m_s = +\frac{1}{2} \right\rangle \quad (14.47)$$

is the function

$$\frac{1}{\sqrt{3}} \left| m_\ell = 0, m_s = -\frac{1}{2} \right\rangle - \sqrt{\frac{2}{3}} \left| m_\ell = -1, m_s = +\frac{1}{2} \right\rangle, \quad (14.48)$$

which yields the basis functions for the $|j = 1/2, m_j = -1/2\rangle$ state:

$$\frac{1}{\sqrt{3}} |L_z \downarrow - (L_x - iL_y) \uparrow\rangle. \quad (14.49)$$

Similarly the basis function for the $|j = 1/2, m_j = +1/2\rangle$ state can be found by application of the raising operators J_+ and $(L_+ + S_+)$ to the $|j = 1/2, m_j = -1/2\rangle$ state, or alternatively by requiring orthogonality to the $|j = 3/2, m_j = +1/2\rangle$ state. Applying the raising operator to the state (14.48) yields

$$\begin{aligned} \frac{1}{\sqrt{3}} \left| m_\ell = 0, m_s = +\frac{1}{2} \right\rangle - \sqrt{\frac{2}{3}} \left| m_\ell = +1, m_s = -\frac{1}{2} \right\rangle \\ = \frac{1}{\sqrt{3}} [(L_x + iL_y) \downarrow - L_z \uparrow], \end{aligned} \quad (14.50)$$

which is seen to be orthogonal to

$$\frac{1}{\sqrt{6}}[(L_x + iL_y) \downarrow + 2L_z \uparrow]. \quad (14.51)$$

In finding the basis functions for $\Gamma_8^+(\Gamma_{15}^+)$ we have made use of the symmetry properties of the angular momentum operators. As far as the symmetry properties are concerned, it makes no difference whether \mathbf{L} is an angular momentum function or an electronic energy band wave function with Γ_{15}^+ symmetry. This concept allows us to write down wave functions with Γ_8^+ symmetry derived from other single group states, and examples of such results are given in Sect. 14.7, and others are taken from the literature [47] or elsewhere (see also Appendix D for tables of these coupling coefficients).

14.7 Basis Functions for Other Γ_8^+ States

Basis functions for the Γ_8^\pm state derived from $\Gamma_8^-(\Gamma_{15}^-)$, $\Gamma_8^+(\Gamma_{25}^+)$, $\Gamma_8^-(\Gamma_{25}^-)$, etc. can be found from $\Gamma_8^+(\Gamma_{15}^+)$ and $\Gamma_6^+(\Gamma_{15}^+)$, as explained below. To obtain the basis functions for $\Gamma_8^-(\Gamma_{15}^-)$, all we have to do is to replace

$$L_x, L_y, L_z \rightarrow x, y, z$$

in (14.41) of Sect. 14.6. This set of basis functions is also considered in Sect. 14.8 using tables available from the literature. Likewise to obtain $\Gamma_8^+(\Gamma_{25}^+)$, we have to replace

$$L_x, L_y, L_z \rightarrow \varepsilon_x, \varepsilon_y, \varepsilon_z,$$

where $\varepsilon_x = yz$, $\varepsilon_y = zx$, $\varepsilon_z = xy$. By using this prescription, the basis functions for Γ_8^\pm will be of the same form for all symmetry-related partners, whether the basis functions are derived from a Γ_{15}^\pm or a Γ_{25}^\pm single group representation. This correspondence is a highly desirable feature for working practical problems.

We note that the $\Gamma_8^+(\Gamma_{12}^+)$ representation can also be produced by considering the electron spin for a Γ_{12}^+ spinless level: $\Gamma_6^+ \otimes \Gamma_{12}^+ = \Gamma_8^+$. We can always make a set of four basis functions for this representation out of $f_1 \uparrow, f_1 \downarrow, f_2 \uparrow, f_2 \downarrow$ where $f_1 = x^2 + \omega y^2 + \omega^2 z^2$, $f_2 = f_1^*$ and $\omega = \exp(2\pi i/3)$. This makes up a perfectly good representation, but the actual functions that are partners look very different from those of $\Gamma_8^+(\Gamma_{15}^+)$ or $\Gamma_8^+(\Gamma_{25}^+)$. We can, however, make a unitary transformation of these four functions so that they look like the $\Gamma_8^+(\Gamma_{15}^+)$ set.

We can make use of these double group basis functions in many ways. For example, these basis functions are used to determine the nonvanishing

$\mathbf{k} \cdot \mathbf{p}$ matrix elements ($u_{n,0}^{\Gamma_i} | \mathcal{H}' | u_{n,0}^{\Gamma_j}$) (see Chap. 15 and (15.12)). These basis functions also determine which of the nonvanishing matrix elements are equal to each other for a given group of the wave vector.

One technique that can be used to determine the number of nonvanishing matrix elements in cases involving multidimensional representations is as follows. If the relevant matrix element is of the form $(\Gamma_i | I_{\text{interaction}} | \Gamma_j)$ then the *number of independent matrix elements* is the number of times the identity representation (Γ_1^+) is contained in the triple direct product $\Gamma_i \otimes \Gamma_{\text{interaction}} \otimes \Gamma_j$. For example, the direct product of the matrix element $(\Gamma_1^+ | I_{15}^- | \Gamma_{15}^-)$ is

$$\Gamma_1^+ \otimes \Gamma_{15}^- \otimes \Gamma_{15}^- = \Gamma_1^+ + \Gamma_{12}^+ + \Gamma_{15}^+ + \Gamma_{25}^+, \quad (14.52)$$

and since all nonvanishing matrix elements must be invariant under all symmetry operations of the group, only the Γ_1^+ term leads to a nonvanishing matrix element. This triple direct product then tells us that of the nine possible combinations of partners, there is only one independent nonvanishing matrix element, and therefore all nine possible combinations of partners must be related to this nonvanishing matrix element.

For the case of double groups, the matrix element $(\Gamma_6^+ | I_{15}^- | \Gamma_6^-)$ has $2 \times 3 \times 2 = 12$ possible combinations. Now $\Gamma_6^+ \otimes \Gamma_{15}^- \otimes \Gamma_6^- = \Gamma_1^+ + \Gamma_{15}^+ + \Gamma_{12}^+ + \Gamma_{15}^+ + \Gamma_{25}^+$, so that once again there is only one independent matrix element. Finally, for the case $(\Gamma_6^+ | I_{15}^- | \Gamma_8^-)$ there are 24 possible combinations. The direct product $\Gamma_6^+ \otimes \Gamma_{15}^- \otimes \Gamma_8^- = \Gamma_1^+ + \Gamma_2^+ + \Gamma_{12}^+ + 2\Gamma_{15}^+ + 2\Gamma_{25}^+$, and once again there is one independent matrix element. Furthermore, if Γ_6^- and Γ_8^- are both related through a Γ_{15}^- interaction term, then the *same independent matrix element* applies to both $(\Gamma_6^+ | I_{15}^- | \Gamma_6^-)$ and $(\Gamma_6^+ | I_{15}^- | \Gamma_8^-)$.

14.8 Comments on Double Group Character Tables

At this point, it is important to address the reader to Appendix D, which contains much information and many illustrative tables pertinent to double groups. This appendix provides an interface between this chapter and the literature [48, 54] and various sources of information about double groups.

In dealing with electronic energy bands for which the spin-orbit interaction is included, we use the $|j l s m_j\rangle$ representation, and this in general requires a transformation from the basis functions in the $|\ell s m_\ell m_s\rangle$ representation to the $|j l s m_j\rangle$ representation. Table D.4 in Appendix D gives us the following relations between the pertinent basis functions for the two representations for the double group O_h :

$$\begin{aligned}
\psi_{-1/2}^6 &= \left| \frac{1}{2}, -\frac{1}{2} \right\rangle = -(i/\sqrt{3})(u_x^4 - iu_y^4) \uparrow + (i/\sqrt{3})u_z^4 \downarrow \\
\psi_{1/2}^6 &= \left| \frac{1}{2}, \frac{1}{2} \right\rangle = -(i/\sqrt{3})(u_x^4 + iu_y^4) \downarrow - (i/\sqrt{3})u_z^4 \uparrow \\
\psi_{-3/2}^8 &= \left| \frac{3}{2}, -\frac{3}{2} \right\rangle = (i/\sqrt{2})(u_x^4 - iu_y^4) \downarrow \\
\psi_{-1/2}^8 &= \left| \frac{3}{2}, -\frac{1}{2} \right\rangle = (i/\sqrt{6})(u_x^4 - iu_y^4) \uparrow + (i\sqrt{2}/\sqrt{3})u_z^4 \downarrow \\
\psi_{1/2}^8 &= \left| \frac{3}{2}, \frac{1}{2} \right\rangle = -(i/\sqrt{6})(u_x^4 + iu_y^4) \downarrow + (i\sqrt{2}/\sqrt{3})u_z^4 \uparrow \\
\psi_{3/2}^8 &= \left| \frac{3}{2}, \frac{3}{2} \right\rangle = -(i/\sqrt{2})(u_x^4 + iu_y^4) \uparrow .
\end{aligned} \tag{14.53}$$

In Table D.4, Γ_{15}^- is denoted by Γ_4 , and (u_x^4, u_y^4, u_z^4) are the three partners of Γ_4 , while the spinor partners are denoted by $\uparrow = v_{1/2}^6$ and $\downarrow = v_{-1/2}^6$, thus constituting the $|\ell s m_\ell m_s\rangle$ representations. The linear combinations given in (14.53) and written above are basically the *Clebsch–Gordan coefficients* in quantum mechanics [20]. We make use of these equations in Sect. 14.9 when we discuss the introduction of spin and the spin–orbit interaction into the plane wave relations describing the energy eigenvalues and eigenfunctions of the empty lattice for an electron with spin.

Table D.1 gives the point group character tables for group O and group T_d including double groups, while Table D.7 gives the compatibility relations showing the decomposition of the irreducible representations of T_d and O into the irreducible representations of the appropriate lower symmetry groups. Note in Table D.7 that E refers to the electric field and H to the magnetic field. The table can be used for many applications, such as finding the resulting symmetries under crystal field splittings as for example $O_h \rightarrow D_3$ (see Sect. 14.4). The decomposition of the irreducible representations of the full rotation group into irreducible representations of groups O and T_d for the s, p, d, \dots functions, etc. is given in Tables D.8 and D.9. Note that all the irreducible representations of the full rotation group D_j^\pm are listed, with the \pm sign denoting the parity (even or odd under inversion) and the subscript giving the angular momentum quantum number (j), so that the dimensionality of the irreducible representation D_j^\pm is $(2j + 1)$.

14.9 Plane Wave Basis Functions for Double Group Representations

In Chap. 12 we discussed the nearly free electron approximation for the energy bands in crystalline solids, neglecting the electron spin. In this case, the

electron wave functions were expressed in terms of symmetrized linear combinations of plane waves transforming according to irreducible representations of the group of the wave vector. In the present section, we extend the presentation in Chap. 12 by giving an explicit example for O_h symmetry (space group #221 for the simple cubic lattice) focusing on the plane wave solutions at $k = 0$ for the corresponding situation where the spin of the electron is included and the wave functions are described in terms of the double group irreducible representations.

It is relatively simple to include the effect of the electron spin for the irreducible representations Γ_1^\pm and Γ_2^\pm because there are no splittings induced by the spin-orbit coupling. Thus the basis functions in this case are simple product functions given by $\Gamma_6^\pm = \Gamma_1^\pm \otimes \Gamma_6^+$ and $\Gamma_7^\pm = \Gamma_2^\pm \otimes \Gamma_6^+$ or more explicitly

$$\begin{aligned}\Psi_{\Gamma_6^\pm}(\mathbf{K}_{n_i}) &= \psi_{\Gamma_1^\pm}(\mathbf{K}_{n_i}) \begin{pmatrix} \alpha \\ \beta \end{pmatrix} \\ \Psi_{\Gamma_7^\pm}(\mathbf{K}_{n_i}) &= \psi_{\Gamma_2^\pm}(\mathbf{K}_{n_i}) \begin{pmatrix} \alpha \\ \beta \end{pmatrix},\end{aligned}\quad (14.54)$$

in which the \mathbf{K}_{n_i} denote reciprocal lattice vectors while $\psi_{\Gamma_1^\pm}(\mathbf{K}_{n_i})$ and $\psi_{\Gamma_2^\pm}(\mathbf{K}_{n_i})$ denote the symmetrized plane wave combinations considered in Chap. 12, but in that case ignoring the effect of the electron spin, while α and β here denote spin up and spin down functions, respectively, which form partners of the Γ_6^+ double group irreducible representation.

For the degenerate plane wave combinations, such as those with Γ_{12}^\pm , Γ_{15}^\pm and Γ_{25}^\pm symmetries, one method to find an appropriate set of basis functions when the electron spin is included is to use the tables presented in Appendix D. For example, basis functions for the four partners for $\Gamma_8^\pm = \Gamma_3^\pm \otimes \Gamma_6^+$ can be found in the Table D.5. Consider that the functions u_1^3, u_2^3 for Γ_3 in this table transform as

$$\begin{aligned}u_1^3 &\propto 3z^2 - r^2 \\ u_2^3 &\propto \sqrt{3}(x^2 - y^2)\end{aligned}\quad (14.55)$$

and the spinor functions are given by

$$\begin{aligned}v_{+1/2}^6 &\propto \alpha \\ v_{-1/2}^6 &\propto \beta.\end{aligned}\quad (14.56)$$

Then the application of Table D.5 gives

$$\Psi_{\Gamma_8^\pm}(\mathbf{K}_{n_i}) = \frac{1}{\sqrt{2}} \begin{pmatrix} \sqrt{3}(x^2 - y^2)\alpha \\ (3z^2 - r^2)\beta \\ -(3z^2 - r^2)\alpha \\ -\sqrt{3}(x^2 - y^2)\beta \end{pmatrix}.\quad (14.57)$$

A more symmetric set of basis functions for $\Gamma_8^\pm = \Gamma_{12}^\pm \otimes \Gamma_6^\pm$ is

$$\Psi_{\Gamma_8^\pm}(\mathbf{K}_{n_i}) = \frac{1}{\sqrt{2}} \begin{pmatrix} [\omega^2 \psi_{\Gamma_{12}^\pm}^*(\mathbf{K}_{n_i}) + \omega \psi_{\Gamma_{12}^\pm}(\mathbf{K}_{n_i})] \alpha \\ -i[\omega^2 \psi_{\Gamma_{12}^\pm}^*(\mathbf{K}_{n_i}) - \omega \psi_{\Gamma_{12}^\pm}(\mathbf{K}_{n_i})] \beta \\ i[\omega^2 \psi_{\Gamma_{12}^\pm}^*(\mathbf{K}_{n_i}) - \omega \psi_{\Gamma_{12}^\pm}(\mathbf{K}_{n_i})] \alpha \\ -[\omega^2 \psi_{\Gamma_{12}^\pm}^*(\mathbf{K}_{n_i}) + \omega \psi_{\Gamma_{12}^\pm}(\mathbf{K}_{n_i})] \beta \end{pmatrix}, \quad (14.58)$$

in which $\psi_{\Gamma_{12}^+}(\mathbf{K}_{n_i}) = x^2 + \omega y^2 + \omega^2 z^2$ and $\psi_{\Gamma_{12}^+}^*(\mathbf{K}_{n_i}) = x^2 + \omega^2 y^2 + \omega z^2$.

Since the three-dimensional levels Γ_{15}^\pm and Γ_{25}^\pm split under the spin–orbit interaction

$$\Gamma_{15}^\pm \otimes D_{1/2} = \Gamma_6^\pm + \Gamma_8^\pm$$

$$\Gamma_{25}^\pm \otimes D_{1/2} = \Gamma_7^\pm + \Gamma_8^\pm$$

the basis functions for these levels are somewhat more complicated, but the coupling coefficients can be found in Table D.4 for the case of $\Gamma_{15}^\pm \otimes D_{1/2}$ and in Table D.6 for the case of $\Gamma_{25}^\pm \otimes D_{1/2}$. In these tables, (u_x^4, u_y^4, u_z^4) and (u_x^5, u_y^5, u_z^5) are the three partners of Γ_{15}^\pm (Γ_4) and Γ_{25}^\pm (Γ_5), respectively, and from these tables we obtain for the twofold levels:

$$\begin{aligned} \Psi_{\Gamma_6^\pm}(\mathbf{K}_{n_i}) &= \frac{1}{\sqrt{3}} \begin{pmatrix} [-i(\psi_{\Gamma_{15}^\pm}^x(\mathbf{K}_{n_i}) - i\psi_{\Gamma_{15}^\pm}^y(\mathbf{K}_{n_i})) \alpha + i\psi_{\Gamma_{15}^\pm}^z(\mathbf{K}_{n_i}) \beta] \\ [-i(\psi_{\Gamma_{15}^\pm}^x(\mathbf{K}_{n_i}) + i\psi_{\Gamma_{15}^\pm}^y(\mathbf{K}_{n_i})) \beta - i\psi_{\Gamma_{15}^\pm}^z(\mathbf{K}_{n_i}) \alpha] \end{pmatrix} \\ \Psi_{\Gamma_7^\pm}(\mathbf{K}_{n_i}) &= \frac{1}{\sqrt{3}} \begin{pmatrix} [-i(\psi_{\Gamma_{25}^\pm}^x(\mathbf{K}_{n_i}) - i\psi_{\Gamma_{25}^\pm}^y(\mathbf{K}_{n_i})) \alpha + i\psi_{\Gamma_{25}^\pm}^z(\mathbf{K}_{n_i}) \beta] \\ [-i(\psi_{\Gamma_{25}^\pm}^x(\mathbf{K}_{n_i}) + i\psi_{\Gamma_{25}^\pm}^y(\mathbf{K}_{n_i})) \beta - i\psi_{\Gamma_{25}^\pm}^z(\mathbf{K}_{n_i}) \alpha] \end{pmatrix}. \end{aligned} \quad (14.59)$$

Problem 14.3 considers the corresponding fourfold levels obtained from taking the direct products of $\Gamma_{15}^\pm(\Gamma_4^\pm) \otimes \Gamma_6^\pm$ and $\Gamma_{25}^\pm(\Gamma_5^\pm) \otimes \Gamma_6^\pm$.

14.10 Group of the Wave Vector for Nonsymmorphic Double Groups

In the case of nonsymmorphic space groups, we found in Sect. 12.5 that bands are often required to stick together at certain high symmetry points on the Brillouin zone boundary where the structure factor vanishes. In Sect. 12.5 it was explicitly shown that for the diamond structure the nondegenerate Δ_1

and Δ_2' levels come into the X point with equal and opposite nonzero slopes, so that in the extended Brillouin zone, the $E(\mathbf{k})$ curves together with all their derivatives, pass through the X point continuously as they interchange their symmetry designations. It was shown in Sect. 12.5 that the physical basis for bands sticking together in this way is that the structure factor vanishes. In such cases it is as if there were no Brillouin zone boundary so that the energy eigenvalues continue through the symmetry point without interruption.

In this section, we consider the corresponding situation including the electron spin and the spin-orbit interaction. Here we explicitly illustrate the sticking together of energy bands in terms of another space group #194 for the hexagonal close packed structure. Another objective of this section is to gain further experience with using double group irreducible representations. Space group #194 was previously discussed in Problems 9.6 and 10.6 and in Sect. 11.4.3 in relation to the lattice modes in graphite. In the case of lattice modes, we only make use of the single group representations. Mention of space group #194 was also made in Sect. 12.5 in connection with bands sticking together at the zone boundary in cases where the structure factor vanishes for nonsymmorphic groups, but in Sect. 12.5 the electron spin and the spin-orbit interaction was neglected. We here consider the case where energy bands for the nonsymmorphic hexagonal close packed lattice stick together and the spin-orbit interaction is included [26] so that double groups must be considered.

Let us consider the wave vector to going from a high symmetry point (Γ) (see Fig. C.7) to a lower symmetry point (Δ) to the point A at the BZ boundary. The double group character tables for these three high symmetry points Γ , Δ and A are found in Tables D.10, D.11 and D.13, respectively. At the A point there are six classes for the group of the wave vector and six irreducible representations, three of which are ordinary irreducible representations Γ_1^A , Γ_2^A , Γ_3^A and three of which are double group representations (Γ_4^A , Γ_5^A , Γ_6^A).

The compatibility relations between the irreducible representations at A and at Δ :

$$\begin{array}{cccccc}
 \text{(A)} & 1 & 2 & 3 & 4+5 & 6 \\
 & \downarrow & \downarrow & \downarrow & \downarrow & \downarrow \\
 \text{(\Delta)} & (1+3) & (2+4) & (5+6) & 2(9) & (7+8)
 \end{array}$$

show that in the vicinity of the A point, we have band crossings for all the single group bands with A_1 , A_2 and A_3 symmetry. These band crossings, shown in Fig. 14.5, are based on these compatibility relations. The energy bands pass through the A point without interruption and merely change their symmetry designations, as for example $\Delta_1 \rightarrow A_1 \rightarrow \Delta_3$. Bands for the doubly degenerate double group irreducible representations Δ_7 and Δ_8 stick together as an A_6 band at the A point. At the A point ($k_z = \pi/c$) the phase factor $\exp[i(c/2)k_z]$, associated with the symmetry operations containing $\tau = (c/2)((0, 0, 1)$ such as $\{C_6|\tau\}$, becomes $e^{i\pi/2} = i$. Energy bands with double group representations A_4 and A_5 have complex characters and are complex conjugates of each

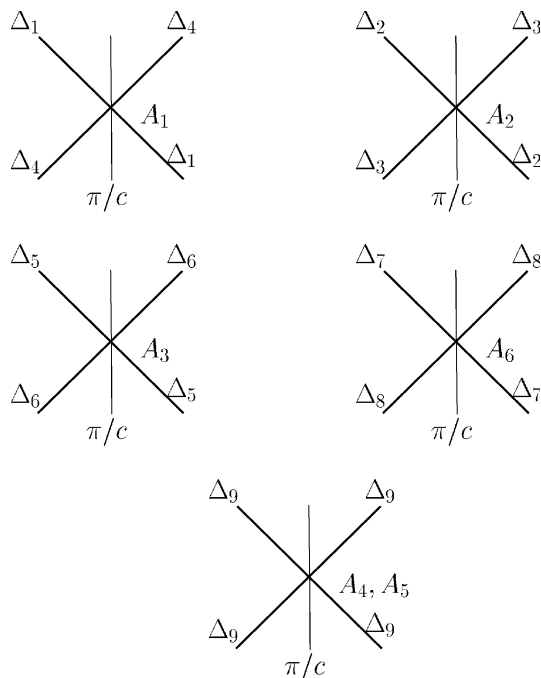


Fig. 14.5. Energy band dispersion relations for various irreducible representations for group #194 near the A point. The energy bands go through the A point without interruption because of the vanishing structure factor at the A point. Note that A_4 , A_5 , A_6 , Δ_7 , Δ_8 and Δ_9 are double group representations. The A_4 and A_5 levels stick together because of time reversal symmetry discussed in Chap. 16

other. In Chap. 16 we will see that such bands stick together because of time reversal symmetry. Thus two Δ_9 levels come into the A point to form $A_4 + A_5$ levels and leave the A point with the same Δ_9 symmetry (see Fig. 14.5).

Selected Problems

- 14.1.** (a) Following the procedure in Sect. 14.3, find the double group character table for the point group D_6 . First find the number of classes and the number of irreducible representations. Then identify the classes as listed in the character table, and the dimensionality of each irreducible representation. Finally find the entries in the character table.
- (b) Use the results in (a) to obtain the double group character table for the group of the wave vector at $k = 0$ for space group #194 which is a nonsymmorphic group. Check your results against Table D.10.
- (c) To which double group states do the states Γ_7^+ , Γ_8^+ , and Γ_9^+ couple optically through electric dipole transitions?

14.2. Consider an Er^{3+} rare earth ion entering an insulating ionic crystal in a position with point group symmetry D_{4h} .

- (a) Find the double group irreducible representations of the crystal field (D_{4h} point group symmetry) corresponding to the ground state configuration for the free ion. Compare with the crystal field splitting that would occur for icosahedral point group symmetry I_h .
- (b) Use Hund's rules (see page 404 of Ref. [45]) to identify the lowest energy optical transitions that can be induced from the ground state level of the free Er^{3+} ion. Using group theory, find the lowest energy transitions expected for an Er^{3+} ion in a crystal with D_{4h} point group symmetry.
- (c) What changes in the spectra (b) are expected to occur if a stress is applied along the fourfold symmetry axis? in the direction along a twofold axis perpendicular to the fourfold axis?
- (d) Now suppose that a Dy^{3+} rare earth ion is introduced into the same lattice instead of the Er^{3+} ion. What are the symmetry types for levels to which optical transitions can be induced from a multiplet corresponding to the ground state level of the free Dy^{3+} ion. (Use Hund's rule to obtain the ground state energies.) Work the problem only for the D_{4h} point group symmetry. Comment on the expected differences in the optical spectrum for the Dy^{3+} and the Er^{3+} ions in part (c).

14.3. Using the linear combinations for plane waves given in Chap. 12 and the coupling coefficients in Appendix D (see Sect. 14.9), find the linear combination of the appropriate partners for $\Gamma_8^\pm(\mathbf{k}_{n_i})$ for the fourfold levels obtained from $\Gamma_5^+ \otimes \Gamma_6^+$ for a material crystallizing in the simple cubic structure.